

A direct borohydride—Acid peroxide fuel cell

C. Ponce de León ^a, F.C. Walsh ^{a,*}, A. Rose ^b, J.B. Lakeman ^{a,b}, D.J. Browning ^b, R.W. Reeve ^b

^a *Electrochemical Engineering Group, School of Engineering Sciences, University of Southampton, Highfield, Southampton SO17 1BJ, UK*

^b *Physical Sciences Department, Building 246, Dstl Porton Down, Salisbury SP4 0QR, UK*

Received 20 July 2006; received in revised form 24 October 2006; accepted 27 October 2006

Available online 4 December 2006

Abstract

A fuel cell operating with aqueous sodium borohydride and hydrogen peroxide streams, with one, two and four cells (electrode area 64, 128 and 256 cm²) connected in a bipolar mode in a filterpress flow cell is reported. The oxidation of borohydride ion was carried out on Au/C particles supported on a carbon felt electrode while the reduction of hydrogen peroxide was carried out on carbon supported Pt on a carbon paper substrate. Comparable cell potentials and power densities to direct borohydride fuel cells reported in the literature were obtained. The challenges to further development includes: increasing the low current density and avoid decomposition of borohydride and peroxide ions. The maximum power obtained at 20 °C for one, two and four cell stacks was 2.2, 3.2 and 9.6 W (34.4, 25 and 37.5 mW cm⁻², respectively) with cell voltages of 1.06, 0.81 and 3.2 V at current densities of 32, 16 and 12 mA cm⁻², respectively.

© 2006 Elsevier B.V. All rights reserved.

Keywords: Borohydride ion; Carbon felt; Filter-press cell; FM01-LC cell; Hydrogen peroxide; Liquid fuel cell

1. Introduction

Fuel cells have been extensively studied over the last five decades and increasing resources have been used to bring them to a commercial stage and to develop alternative fuels to hydrogen. With the rapid development of different fuel cell designs it is likely that, within the next decade or two, power generation for portable electronic equipment and vehicular transportation will rely on fuel cells for the energy source. Fuels such as natural gas, propane and diesel have been considered but these fuels need to be reformed to produce hydrogen [1], which could reduce the need for high pressure storage tanks. Serious questions remain concerning: (a) the reliability of these systems, (b) safety during storage and (c) problems of supplying flammable, gaseous fuels.

An alternative fuel should include reactants susceptible to direct oxidation without causing passivation of the anode. Such fuels are difficult to find, especially if large molecules are used. If partial oxidation occurs, large anodic overpotentials might result. It has been claimed that hydrocarbon fuels can be used directly in solid oxide fuel cells (SOFC) [2] but direct oxidation

of hydrocarbons involves several mechanistic steps and is prone to electrode passivation [3,4].

These concerns have stimulated research into alternative fuels such as liquid methanol, which has been widely studied in the direct methanol fuel cells (DMFC). Although the anode becomes poisoned during the oxidation process, and methanol crossover through the membrane reduces the efficiency, significant advances have been made to improve the performance of the DMFC [5–7]. More recently, sodium borohydride, typically available as a solid or as a 30% solution in concentrated aqueous sodium hydroxide has been considered as part of the continuous development of alternative high power energy fuel cells for portable applications and underwater vehicles. The development of fuel cells operating with other fuel than hydrogen is important in order to avoid potential hazardous conditions during long-term operations. The borohydride ion has been investigated both as a hydrogen storage medium [8] and as a fuel that can be directly oxidised at the anode surface [9,10], i.e. in the direct borohydride fuel cell (DBFC). Both systems would reduce the problem of specialised pressure storage vessels to externally contain hydrogen.

Ideally, a direct oxidation of the borohydride ion in an alkaline medium involves the transfer of eight electrons at an equilibrium potential of -1.24 versus SHE [11], which, in combination with the reduction of oxygen, gives a theoretical equilibrium cell

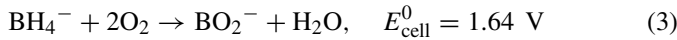
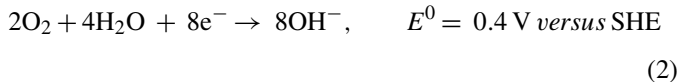
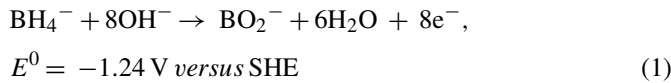
* Corresponding author. Tel.: +44 2380 598752.

E-mail address: F.C.Walsh@soton.ac.uk (F.C. Walsh).

Nomenclature

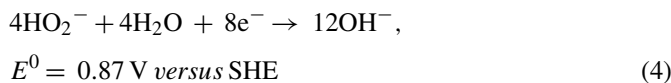
| | |
|----------------------|--|
| E_A | anode potential (V) |
| E_C | cathode potential (V) |
| E^0 | standard potential (V) |
| E_A^e | equilibrium potential of the anodic reaction (V) |
| E_C^e | equilibrium potential of the cathodic reaction (V) |
| E_{cell}^0 | standard cell potential (V) |
| I | current (mA) |
| j | current density (mA cm^{-2}) |
| P_{cell} | power density of the cell (W cm^{-2}) |
| R | resistance (Ω) |
| T | temperature ($^{\circ}\text{C}$) |
| <i>Greek letters</i> | |
| η_A | overpotential at the anode (V) |
| η_C | overpotential at the cathode (V) |

potential of 1.64 V:



This process is shown in Fig. 1a.

The use of hydrogen peroxide instead of oxygen as an oxidant can yield higher cell potential values, its use has been implemented with magnesium [12] and aluminium [13] anodes in a number of prototype batteries for undersea water vehicles, and in borohydride fuel cells [14,15]. Hydrogen peroxide is attractive choice for these applications and is comparatively safe, stable as 35% solution in water, is not toxic and can produce water from its oxidation. The disadvantages of hydrogen peroxide are: lower specific energy in comparison with oxygen and decomposition in the presence of metals, particularly Pt, Pd and Au used as electrocatalysts in fuel cells. Therefore an appropriate cathode should promote the direct reduction of hydrogen peroxide avoiding heterogeneous and surface decomposition to oxygen. Direct oxidation of borohydride ion with hydrogen peroxide in alkaline solution at the cathode [15] is:



The cell reaction in this situation provides a theoretical cell potential of 2.11 V (Fig. 1b):

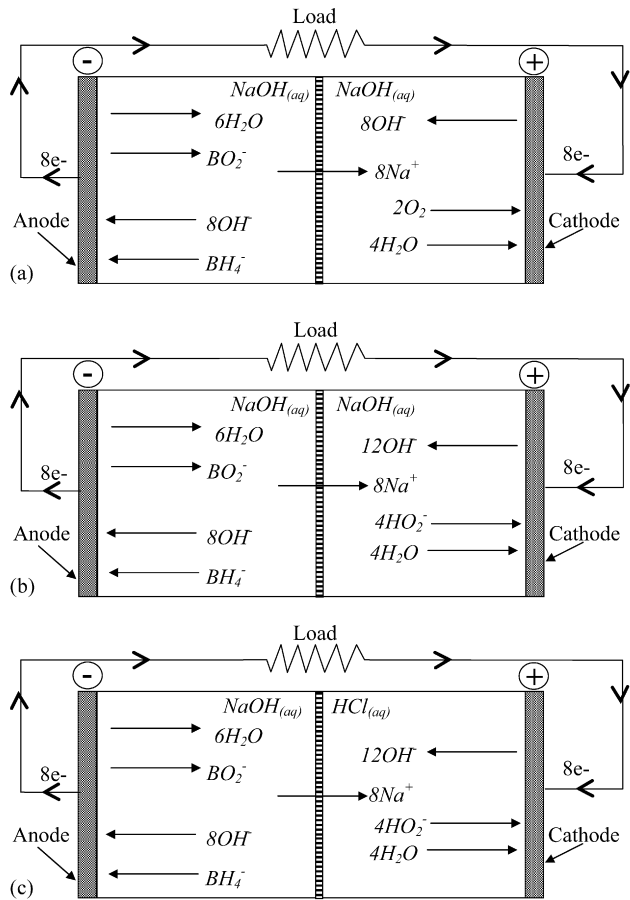
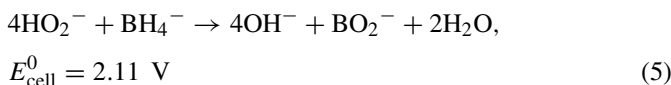
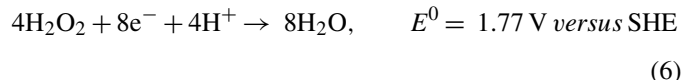


Fig. 1. Types of borohydride fuel cell: (a) with alkaline oxygen reduction, (b) with alkaline hydrogen peroxide reduction at the cathode and (c) with reduction of hydrogen peroxide in an acid electrolyte.

In contrast, the methanol–oxygen and the hydrogen–oxygen fuel cells provide a theoretical equilibrium cell potential, of 1.21 and 1.23 V, respectively [16]. This advantage of borohydride over methanol and hydrogen as an alternative energy source only occurs if both borohydride and peroxide ions react directly at the electrodes. In reality, each half-cell reaction takes up a mixed potential determined by the different redox species involved. The potential of a borohydride anode may be affected by hydrolysis to hydrogen and the borate produced by the direct oxidation. At the cathode, two reactions take place; direct reduction of hydrogen peroxide and reduction of oxygen released from the homogeneous decomposition of peroxide.

Fig. 1c shows the reduction of hydrogen peroxide in acidic media:



The combination of this reaction with the direct oxidation of borohydride provides a cell potential, E_{cell} of 3.01 V, which is 0.9 V higher than the case of hydrogen peroxide reduction in alkaline solution. Despite the number of challenges (heterogeneous decomposition) borohydride–hydrogen peroxide fuel cells offers higher energy output than fuel cells operating with methanol–oxygen and hydrogen–oxygen systems.

In this paper, a direct borohydride fuel cell operating with hydrogen peroxide in an acid electrolyte is reported. A single cell and stacks of two and four cells are considered in terms of their cell potential and power as a function of current density.

2. Experimental details

The electrochemical cell was a filter-press type, laboratory reactor manufactured by INEOS Chlor Chemicals (FM01-LC), which has been characterised in the literature [17–19] and used in electrochemical processing [20–22]. The cell was arranged in a divided configuration, with catholyte and anolyte compartments separated by a NafionTM 117 Na⁺ membrane. The cell unit shown in Fig. 2a comprised of: (a) metal back-plates to collect current from each electrode, (b) electrolyte compart-

ments machined from PTFE, (c) PTFE gaskets, (d) turbulence promoters, (e) PTFE plates of 1 cm thickness and (f) stainless steel plates of 1 cm thickness to hold the electrodes, plates and gaskets. The PTEF turbulence promoter (0.55 cm thick and 16 cm × 4 cm) filled each electrolyte compartment leaving 83% volume porosity (ratio of free volume to total volume of electrolyte compartment) [23]. One-, two- or four cells were connected in the bipolar mode. Fig. 2a shows a single cell with its components while Fig. 2b and c shows the two and four cells arrangements. Each stack of cells shown in Fig. 2 was held together with the stainless steel end plates that were uniformly compressed with eight stainless steel screws to a torque of approximately 25 N m, giving an electrode-membrane gap of 0.55 cm.

PTFE tubing, of 1 mm internal diameter, was fitted at the topside of each electrolyte compartment to serve as a Luggin capillary to monitor the potentials of the anode and cathode. Small gas bubbles of hydrogen and oxygen were observed from the homogeneous decomposition of the anolyte and catholyte respectively. The gas passing through the cell also went through the Luggin capillaries temporarily blocking the ionic contact between the electrodes and their respective reference electrodes. In order to allow continuous measurement, two small peristaltic pumps were connected between the reference electrode reservoirs and the electrolyte tanks to remove gas continuously.

Commercially available electrodes were used; the cathode was a porous carbon paper of 5 cm × 16 cm × 0.03 cm thickness printed with a Pt on carbon black catalyst within a cationic Nafion base ink (Johnson Matthey). The Pt loading was 4.0 mg cm⁻². The anode was a carbon cloth electrode of 5 cm × 16 cm × 0.05 cm thickness with a 10% Au loading on carbon black (Vulcan XC-72), resulting in a 0.5 mg Au cm⁻² loading (E-TEK). Each electrode was in contact with a niobium back plate acting as a current collector. The projected area of each electrode facing the electrolyte was 64 cm² (16 cm × 4 cm), the remaining 0.5 cm on each side of the electrode was used to hold and compress the electrodes to the niobium back plate. The anolyte was 1 dm³ 25% NaBH₄ in 6 mol dm⁻³ NaOH and the catholyte was 1 dm³ 1 mol dm⁻³ H₂O₂ in 1 mol dm⁻³ HCl + 3 mol dm⁻³ NaCl solution, both prepared using freshly deionised water. Each electrolyte was contained in a 2.0 dm³ glass reservoir fitted with a water jacket chamber where the water was circulated and the temperature was controlled by a thermostatic bath (Grant, model LTD6G). The operating temperatures were 20, 40 and 60 °C.

The electrolyte circuit shown in Fig. 3 was constructed from PVC, PVDF and PTFE tubing and fittings. Magnetically coupled, centrifugal pumps (March May model TE-3K-MD) were used to circulate the electrolyte through the cell and the flow rates were measured using variable area polysulfone flowmeters, controlled manually through PVC valves. A flow rate of $95 \pm 5 \text{ L h}^{-1}$ was used in all the experiments corresponding to a mean linear flow velocity of 12.0, 6.0 and 3.0 cm s⁻¹ for the single, two and four cell stacks, respectively.

A programmable electronic load (Kikusui model PLZ334W) was used to test the cell at constant current. The data was

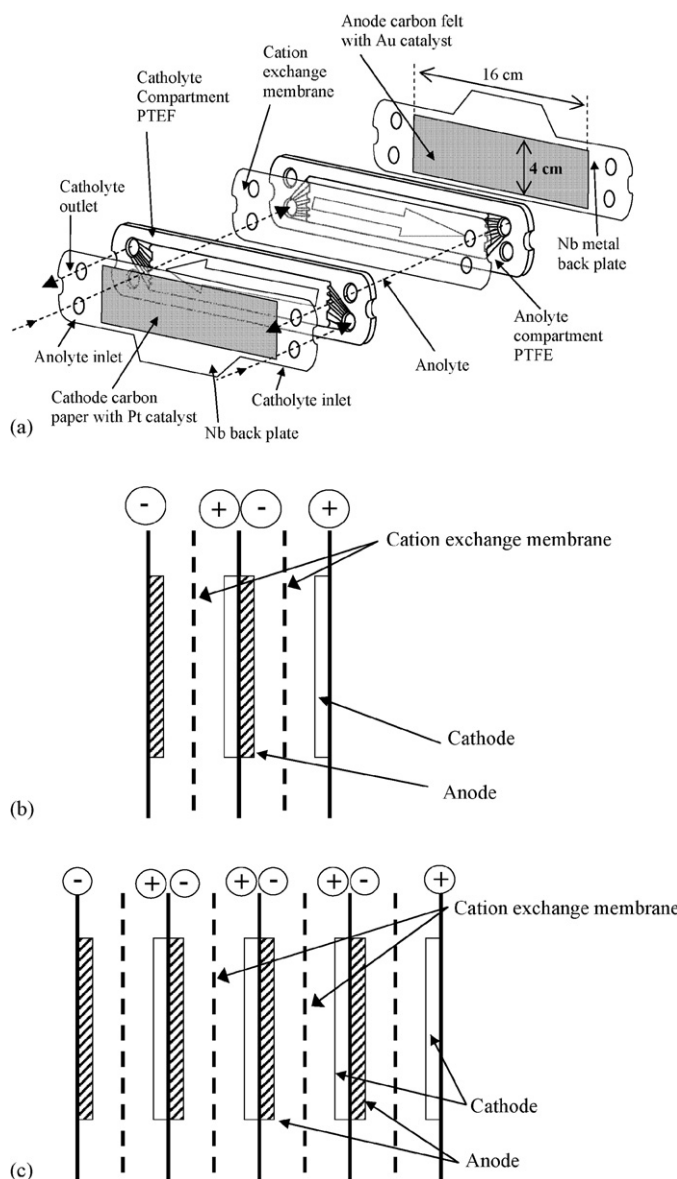


Fig. 2. The flow cell—(a) exploded view of a single FM01-LC cell in the divided single-cell configuration. The main frame, gaskets and turbulence promoter are not shown, (b) two-cell stack and (c) four-cell stack.

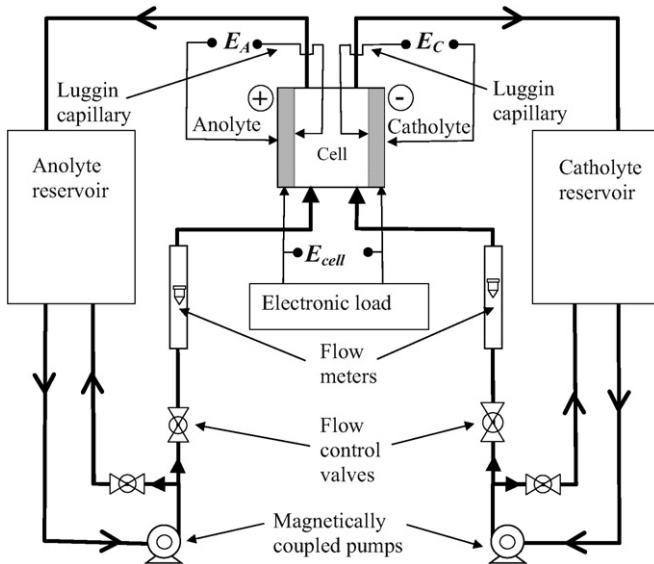


Fig. 3. Electrolyte and electrical circuits.

collected on a PC connected to the electronic load by a USB port. The potentials of the anode and cathode electrodes were measured with saturated calomel electrodes, SCE, fitted in a reservoir connected to the Luggin capillaries from the cell. The SCE potential values were converted to the standard hydrogen electrode scale (0.241 *versus* SHE) in the plots. The potential differences were monitored using a data acquisition card (NI model DAQ 6052). A standard virtual instrument program, run in LabView™ software, was used to acquire the data.

3. Results and discussion

3.1. Voltage and power in a single cell

Fig. 4 shows a plot of both, cell voltage and power density *versus* current density for a single cell operating with 25% NaBH₄ in 6 mol dm⁻³ NaOH in the anolyte and 1 mol dm⁻³ H₂O₂ in 1 mol dm⁻³ HCl + 3 mol dm⁻³ NaCl in the catholyte at 20 °C. The load was applied in steps of 0.25 A within the range of 0–5 A. Each step lasted 1 min and the current was continuously applied from one value to the next without disconnecting the cell. The cell voltage curve shows an open circuit potential (OCP) value of 1.9 V. In acidic solution the theoretical cell potential should be ≈3 V, since the reduction of peroxide in acid is 1.77 V *versus* SHE, as shown in reaction (6). However, the experimental cell potential value is closer to 2.11 V, which is the value of the borohydride–peroxide cell when peroxide is reduced in alkaline solutions as shown in Eq. (4). The cell voltage drops as the current increases; at 10 mA cm⁻², the cell voltage decreased around 0.2 V and continued to decay linearly with current density, showing a strong dependence on the ohmic resistance of the cell. Overpotentials due to kinetic limitations cannot be seen as they are probably masked by IR drop. Mass transport effects are observed above a current density of approximately 50 mA cm⁻². The curve corresponding to the power density *versus* current

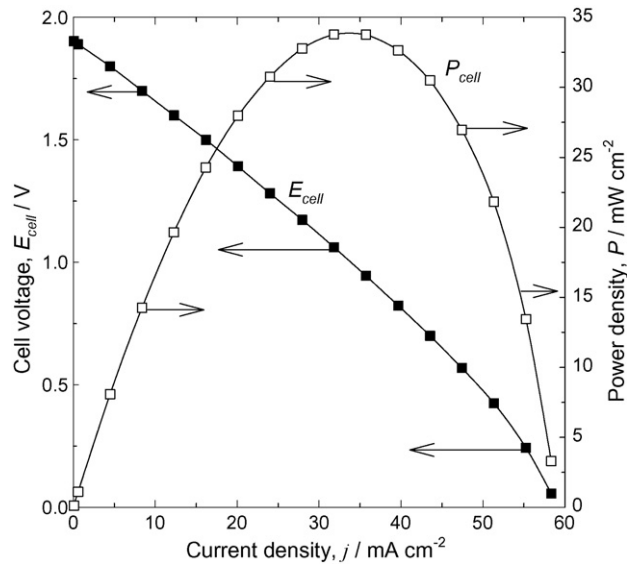


Fig. 4. Cell voltage and power density for a single-cell operating at 20 °C with anolyte consisted of 25% NaBH₄ in 6 mol dm⁻³ NaOH and 1 mol dm⁻³ H₂O₂ in 1 mol dm⁻³ HCl catholyte. Flow rate 95 ± 5 L h⁻¹. Anode of Au on carbon Vulcan XC-72 supported on a carbon felt and Pt cathode on carbon supported on carbon paper.

density shows a maximum point of 34 mW cm⁻² at a current density of 37 mA cm⁻².

Fig. 5 shows the anode E_A , and cathode E_C , potentials measured experimentally and the calculated $E_C - E_A$ value plotted *versus* the current density. For comparison, the experimental cell potential E_{cell} , from Fig. 4 is also included. The cathode potential E_C at zero current is 0.88 V *versus* SHE, which is very close to the theoretical value of the reduction of peroxide in alkaline solution shown in reaction (4). Since the electrolyte used

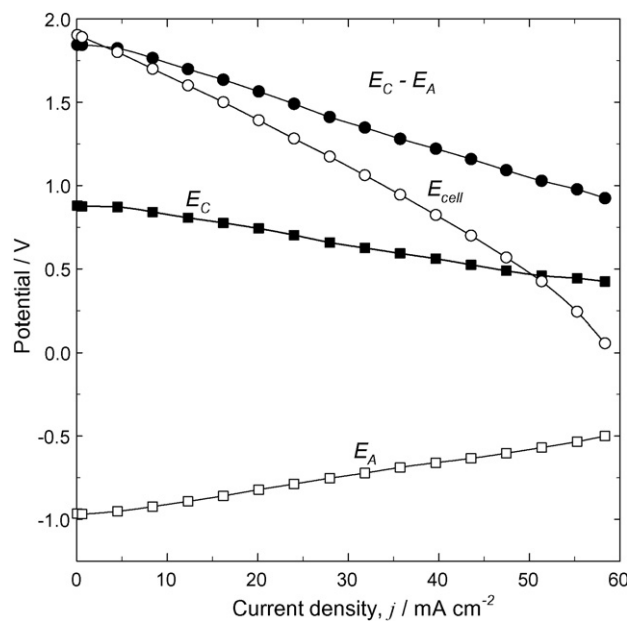


Fig. 5. Cell voltage, E_{cell} , anode potential, E_A , cathode potential, E_C , and $E_C - E_A$ *vs.* current density for the single cell borohydride fuel cell described in Fig. 4. The potentials of the anode and cathode are stated *vs.* SHE.

is 1 mol dm⁻³ of HCl, the potential suggests a mixed reaction involving the reduction of oxygen (0.4 *versus* SHE), generated by the decomposition of peroxide, and the direct reduction of hydrogen peroxide in acid (1.77 *versus* SHE).

The cell potential E_{cell} may be expressed as

$$E_{\text{cell}} = (E_C - E_A) - \sum \text{IR} \quad (7)$$

where the term $\sum \text{IR}$ corresponds to all the potential drops within the cell including membrane, electrolyte and the electrical circuit but excluding the overpotentials of the electrode reactions. The overpotential due to the electrode reaction is included in the terms E_C and E_A that can be written as

$$E_C = E_C^e - \sum \eta_C \quad (8)$$

$$E_A = E_A^e - \sum \eta_A \quad (9)$$

where E_C^e and E_A^e are the equilibrium potentials of the cathodic and anodic reactions according to Eqs. (6) and (1), respectively, and η_A and η_C are the anode and cathode overpotentials, respectively. The cathode potential E_C , dropped linearly to 0.46 V *versus* SHE when the current increased to 60 mA cm⁻². The potential of the anode electrode E_A , at zero current was -0.96 V *versus* SHE, almost 0.280 V higher than the theoretical value of the oxidation of borohydride illustrated in Eq. (1) (-1.24 *versus* SHE). This value probably represents a mixed potential between the direct oxidation of borohydride, the oxidation of hydrogen and the oxidation of borates generated by the homogeneous decomposition of borohydride. The potential of the anode increased to -0.5 V *versus* SHE when the current increased to 60 mA cm⁻². Both potentials E_C and E_A changed with current, showing that the overpotentials η_C and η_A in Eqs. (8) and (9) increased linearly with applied current.

A comparison of the cell potential E_{cell} , and the cell potential calculated from the values of the half cell reactions, $E_C - E_A$, show that E_{cell} drops faster than the cell potential evaluated from the half cell reactions. The difference between the two was small at low current densities but increased with current and at 60 mA cm⁻² the difference was almost 0.870 V. The fact that E_{cell} dropped faster than the calculated $E_C - E_A$ suggest that the term $\sum \text{IR}$ which increased with current does not involve the overpotential of the electrode reactions. This could be due to a change in the electrolyte composition or a resistance to ionic transport within the membrane. Since the current density across the membrane is low compared to those typically encountered in Nafion based electrochemical systems, the membrane could have been partially blocked, since high concentration of the electroactive species is unlikely to decrease in such a short period of time.

3.2. Voltage and power in a single cell with time

Fig. 6a shows the values of E_{cell} , E_A , E_C , and $E_C - E_A$ *versus* time when a current load of 2 A (37 mA cm⁻²) was applied to a single cell. The figure shows that the anode and cathode potentials remained constant for the duration of the experiment (>1 h). The calculated cell potential value from the two half-cell

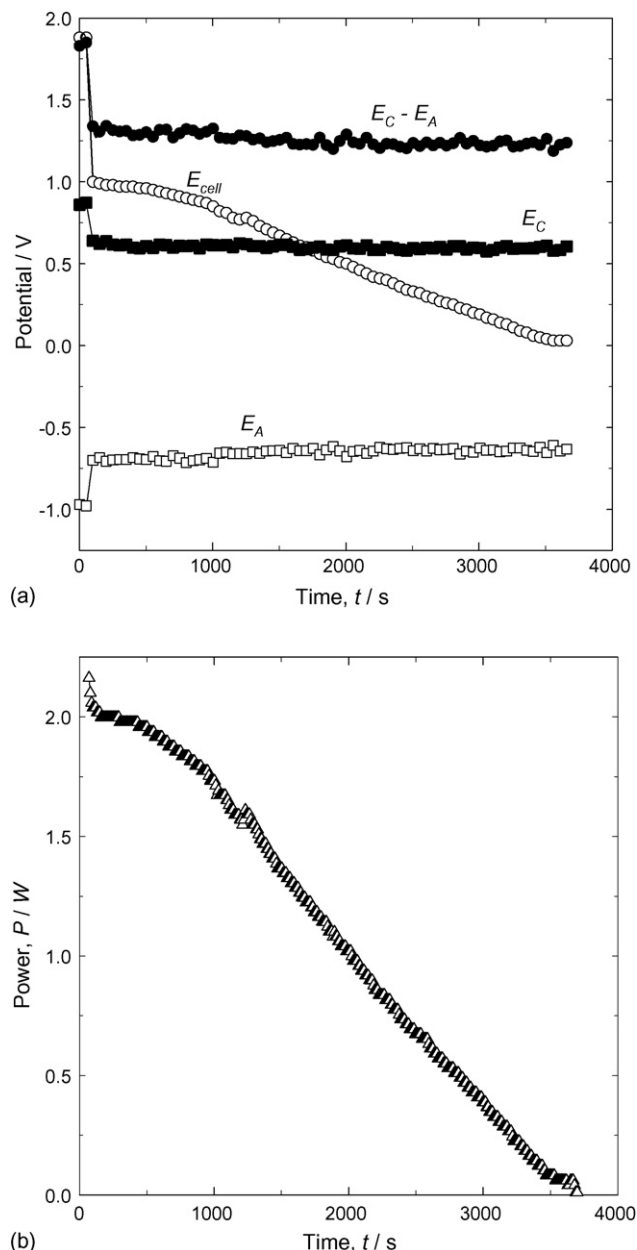
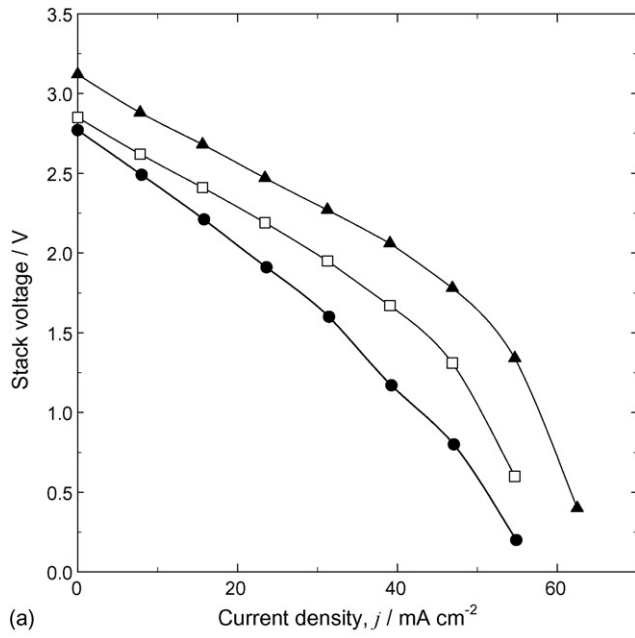
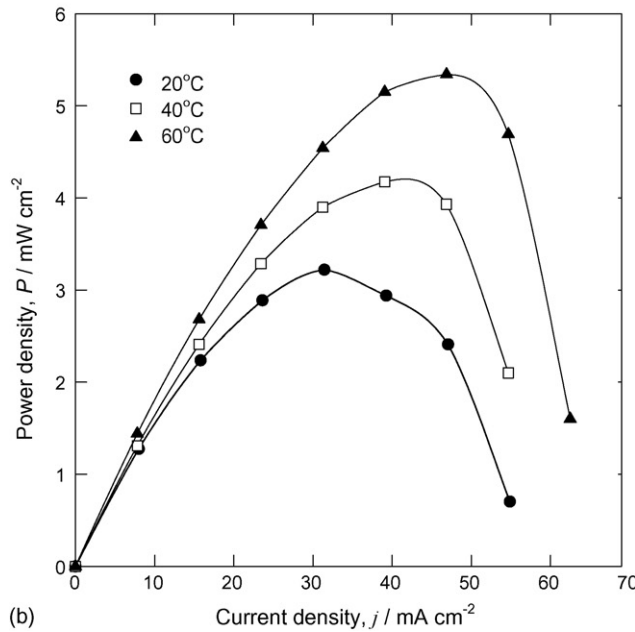


Fig. 6. (a) Cell voltage, E_{cell} , anode potential, E_A , cathode potential, E_C , $E_C - E_A$ and (b) power *vs.* time for a single-cell operating at 20 °C and discharging at a constant current of 2 A (31.2 mA cm⁻²).

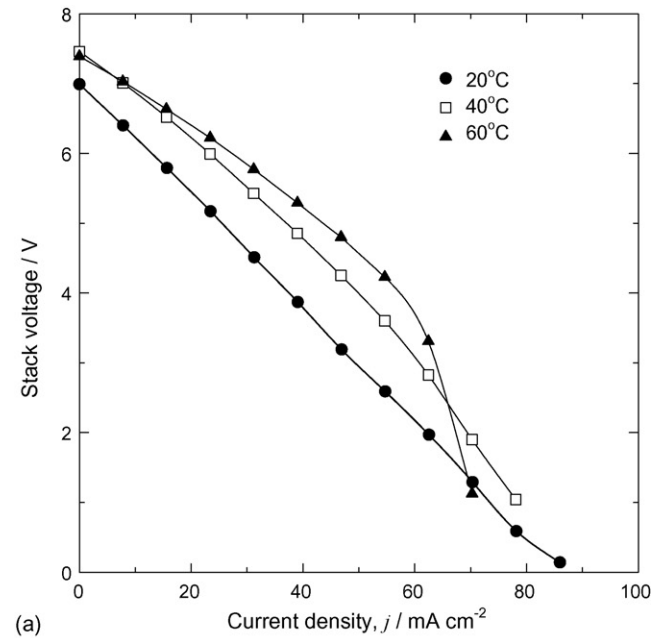
reactions consequently remained constant but the experimental cell potential E_{cell} started to decrease 500 s after the load was applied. The fact that the potential of the two electrode reactions keep a constant value while the cell potential E_{cell} drops, suggests an increase in the ohmic losses through the membrane or through the electrolyte. As in the experiment depicted in Fig. 5, it is likely that the membrane has been mechanically blocked, probably by the products generated from the oxidation of borohydride. Fig. 6b shows the power generated during the application of the 2 A current load to the single cell. The curve shows that the power remains approximately constant during the first 500 s of the experiment, but started to decay linearly, reaching zero power in about 3600 s. This is directly related to the



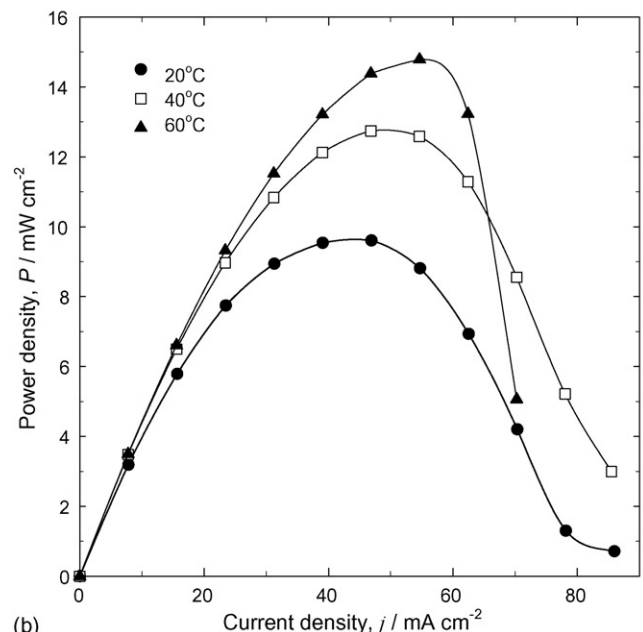
(a)



(b)



(a)



(b)

Fig. 7. (a) Potential and (b) power density for a two-cell stack operating at different temperatures with a mean linear flow velocity of 6 cm s^{-1} . The anolyte consisted of 25% NaBH_4 in 6 mol dm^{-3} NaOH anolyte with Au on carbon Vulcan XC-72 supported on a carbon felt and catholyte of 1 mol dm^{-3} H_2O_2 in 1 mol dm^{-3} $\text{HCl} + 3 \text{ mol dm}^{-3}$ NaCl in contact with Pt/C (supported on carbon paper).

value of the cell potential E_{cell} that, as described above, appears to decay due to an increase of IR drop within the cell.

3.3. Two- and four-cell stacks

Two and four cell stacks were tested with the same electrolyte solutions used for the single cell. The stacks were arranged in the bipolar mode as shown in Fig. 2b and c. Figs. 7a and 8a show the cell potential E_{cell} and Figs. 7b and 8b

Fig. 8. (a) Potential and (b) power density for a four-cell stack operating at different temperatures at a mean linear flow velocity of 3 cm s^{-1} . The anolyte consisted of 25% NaBH_4 in 6 mol dm^{-3} NaOH anolyte with Au on carbon Vulcan XC-72 supported on a carbon felt with a catholyte of 1 mol dm^{-3} H_2O_2 in 1 mol dm^{-3} $\text{HCl} + 3 \text{ mol dm}^{-3}$ NaCl in contact with Pt/C (supported on carbon paper).

show the power *versus* current density obtained from the two stacks at three temperatures; 20, 40 and 60°C. Cell potential and power increase with temperature in both stacks. The data for the open circuit potential E_{OCP} and the maximum power achieved by the single, two and four cells stack are presented in Table 1.

The open circuit potential E_{OCP} , at 20°C increased with the number of cells in the stack. However, the potential in the two and four cell stacks was not equal to twice and four times, respec-

Table 1

Results obtained from a single-, two- and four-cell stack operating with anolyte consisted of 25% NaBH₄ in 6 mol dm⁻³ NaOH and Au on carbon Vulcan XC-72 supported on a carbon felt as anode

| Temperature (°C) | Open circuit voltage, E_{OCP} (V) ($j=0$) | Cell voltage, E_{cell} (V) | Power (W) | Power density, P (mW cm ⁻²) | Current, I (A) | Current density, j (mA cm ⁻²) | Mean linear flow velocity, v (cm s ⁻¹) |
|------------------|---|------------------------------|-----------|---|------------------|---|--|
| Single cell | | | | | | | |
| 20 | 1.90 | 1.06 | 2.2 | 34 | 2.0 | 31.8 | 12 |
| Two-cell stack | | | | | | | |
| 20 | 2.78 | 0.81 | 3.2 | 25 | 2.0 | 16.0 | 6 |
| 40 | 2.85 | 0.89 | 4.2 | 33 | 2.5 | 19.5 | 6 |
| 60 | 3.12 | 0.97 | 5.3 | 42 | 3.0 | 23.5 | 6 |
| Four-cell stack | | | | | | | |
| 20 | 7.0 | 3.20 | 9.6 | 38 | 3.0 | 11.7 | 3 |
| 40 | 7.5 | 4.20 | 12.7 | 50 | 3.0 | 11.7 | 3 |
| 60 | 7.4 | 4.80 | 14.8 | 58 | 3.5 | 13.7 | 3 |

The catholyte was 1 M H₂O₂ in 1 mol dm⁻³ HCl + 3 mol dm⁻³ NaCl in contact with Pt on carbon catalyst supported on carbon paper. The cell potential E_{cell} and currents were recorded at the maximum power achieved. The total area of a single-, two- and four-cell stack was 64, 128 and 256 cm², respectively, and the volumetric flow rate was 95 dm³ h⁻¹ (1.6 dm³ min⁻¹) in all cases.

Table 2

Results taken from the literature for a MEA borohydride fuel cell: (a)–(d) were fabricated with 1 mg cm⁻² Pt/C cathode and anode made of misch metal Ni_{3.55}Al_{0.3}Mn_{0.4}Co_{0.75} alloy (5 mg cm⁻²) on carbon Vulcan XC-72R pasted on carbon paper Toray TGP-H-090

| Example | pH | Peak power density at different temperatures (mW cm ⁻²) | | | | Cell voltage at peak power density at different temperatures (V) | | | |
|---------|------|---|-------|-------|-------|--|-------|-------|-------|
| | | 35 °C | 40 °C | 60 °C | 70 °C | 35 °C | 40 °C | 60 °C | 70 °C |
| (a) | 1.0 | – | 70 | 110 | 130 | – | 1.5 | 1.2 | 0.7 |
| (b) | 0.0 | 112 | 122 | 194 | 236 | 0.9 | 0.89 | 0.98 | 1.1 |
| (c) | 0.5 | 136 | 146 | 260 | 352 | 1.0 | 0.98 | 1.2 | 1.2 |
| Example | pH | Peak power density at different temperatures (mW cm ⁻²) | | | | Cell voltage at peak power density at different temperatures (V) | | | |
| | | 50 °C | 70 °C | 85 °C | – | 50 °C | 70 °C | 85 °C | – |
| (d) | 14.0 | 99 | 150 | 189 | – | 0.59 | 0.50 | 0.56 | – |

The anolyte solution was 10% NaBH₄ in 20% NaOH (a–c) and 30% (d) at 3 mL min⁻¹ and the catholyte was 15%, w/v H₂O₂ acidified with H₂SO₄ (a–c) and 8.9 mol dm⁻³ H₂O₂ (d) at 5 cm³ min⁻¹ [24]. Experiment (d) was carried out with an anolyte consisted on 10% NaBH₄ in 20% NaOH at 0.2 dm³ min⁻¹ and the catholyte was humidified O₂ at 0.2 dm³ min⁻¹. The cathode was a carbon supported Pt catalyst and the anode was an AB₂ alloy: Zr_{0.9}Ti_{0.1}Mn_{0.6}V_{0.2}Co_{0.1}Ni_{1.1} [25].

tively, the value of the single cell potential. The cell voltage losses could be originated from the amount of gas generated by the homogeneous decomposition of the electrolyte or potentially shunts currents associated with the fuel and oxidant through the supporting electrolyte. It is interesting to note that the peak power generated by the single, two and four cell arrangement at 20 °C was 33, 25 and 37 mW cm⁻², respectively, despite the fact that the mean linear flow velocity decreased with the number of cells in the stack, i.e., 12, 6 and 3 cm s⁻¹ for each cell arrangement respectively. Since there is no effect due to the mean linear flow rate of the electrolyte, this might indicate that the reactions were kinetically controlled.

Table 2 shows data reported in the literature for DBFC membrane electrode assemblies (MEA) at 70 °C. Comparison of the results reported in Tables 1 and 2 show that the MEA arrangement produces higher power and current densities than those reported in this work. A possible reason for this could be that the AB₂ and AB₅ anodes used in the experiments reported in Table 2 are more active with respect to the oxidation of borohydride ion than the gold catalyst used in this work. The cited refer-

ences show that the anode potential E_A , remains approximately constant, close to the equilibrium potential of borohydride oxidation, while the cathode potential E_C , drops rapidly when the current density increases up to 500 mA cm⁻². Another important factor is the minimization of the interelectrode gap in the MEA system. The IR drop in the flow cell presented in this work is increased by the gas generated by the homogeneous decomposition of the electrolyte during operation. None of the cited papers mention that the gasses generated from the decomposition of the fuel and oxidant presents an operational problem, despite the use of hydrogen peroxide at a concentration as high as 8.9 mol dm⁻³ [24]. In the present studies, higher concentration of peroxide resulted in more difficult operating conditions as the gas produced was trapped in the pumped circuit and the electrical resistance of the cell increased.

4. Conclusions

1. Single-, two- and four-cell stacks were operated in a flow cell for borohydride oxidation. A maximum power of 14.8 W was

achieved using the four-cell stack at 60 °C, while the two- and single cell stacks achieved 12.7 and 9.6 W, respectively, at the same temperature.

2. Problems faced by this type of fuel cell include: potential (and reactant) losses due to the gas derived from the homogeneous decomposition of the electrolyte, and possibly by the mechanical blockage of the ionic channels of the membrane by the products of the oxidation of borohydride ion.
3. Longer duration experiments are needed, with careful monitoring of pH, and the amount of gasses generated by the homogeneous decomposition of hydrogen peroxide and borohydride ion.
4. Borohydride fuel cells offer a number of opportunities such as: use of surfactants and stabilisers to suppress the heterogeneous decomposition of borohydride and hydrogen peroxide solutions, design of electrode materials specific for the direct oxidation of borohydride and reduction of hydrogen peroxide and development of ion exchange membranes capable of withstanding products from the borohydride oxidation without loss of ion exchange capacity.

Acknowledgements

The authors are grateful to M.G. Medeiros, C.J. Patrissi and R.R. Bessette from the Naval Undersea Warfare Center (NUWC) and to M.L. Anderson from the Office of Naval Research (ONR), for discussions on borohydride fuel cells. The authors also gratefully acknowledge the Office of Naval Research and DSTL for funding this work.

References

- [1] J.D. Holladay, Y. Wang, E. Jones, *Chem. Rev.* 104 (2004) 4767.
- [2] S. McIntosh, R.J. Gorte, *Chem. Rev.* 104 (2004) 4845.
- [3] M. Mogensen, K. Kammer, *Annu. Rev. Mater. Res.* 33 (2003) 321.
- [4] O.A. Marina, M. Mogensen, *Appl. Catal. A, Gen.* 189 (1999) 117.
- [5] F. Maillard, G.-Q. Lu, A. Wieckowski, U. Stimming, *J. Phys. Chem. B* 109 (2005) 16230.
- [6] A.K. Shukla, C.L. Jackson, K. Scott, G. Murgia, *J. Power Sources* 111 (2002) 43.
- [7] D. Buttin, M. Dupont, M. Straumann, R. Gille, J.-C. Dubois, R. Ornelas, G.P. Fleba, E. Ramunni, V. Antonucci, A.S. Arico, P. Creti, E. Modica, M. Pham-Thi, J.-P. Ganne, *J. Appl. Electrochem.* 31 (2001) 275.
- [8] W. Chuan, W. Feng, B. Ying, Y. Baolian, Z. Huamin, *Mater. Lett.* 59 (2005) 1748.
- [9] E. Gyenge, M. Atwan, D. Northwood, *J. Electrochem. Soc.* 153 (2006) A150.
- [10] C. Ponce de León, F.C. Walsh, D. Pletcher, D.J. Browning, J.B. Lakeman, *J. Power Sources* 155 (2006) 172.
- [11] L. Wang, C. Ma, X. Mao, *J. Alloy Compd.* 397 (2005) 313.
- [12] M.G. Medeiros, R.R. Bessette, C.M. Deschenes, C.J. Patrissi, L.G. Carreiro, S.P. Tucker, D.W. Atwater, *J. Power Sources* 136 (2004) 226.
- [13] E.G. Dow, R.R. Bessette, G.L. Seebach, C. Marsh-Orndorff, H. Meunier, J. VanZee, M.G. Medeiros, *J. Power Sources* 65 (1997) 207.
- [14] R.K. Raman, A.K. Shukla, *J. Appl. Electrochem.* 35 (2005) 1157.
- [15] N.A. Choudhury, R.K. Raman, S. Sampath, A.K. Shukla, *J. Power Sources* 143 (2005) 1.
- [16] A.K. Shukla, C.L. Jackson, K. Scott, R.K. Raman, *Electrochim. Acta* 47 (2002) 3401.
- [17] M. Griffiths, C. Ponce de León, F.C. Walsh, *AIChE J.* 51 (2005) 682.
- [18] P. Trinidad, F.C. Walsh, *Electrochim. Acta* 41 (1996) 493.
- [19] C.J. Brown, D. Pletcher, F.C. Walsh, J.K. Hammond, D. Robinson, *J. Appl. Electrochem.* 22 (1992) 613.
- [20] C. Bengoa, A. Montillet, P. Legentilhomme, J. Legrand, *Ind. Eng. Chem. Res.* 39 (2000) 2199.
- [21] D. Szántó, P. Trinidad, F.C. Walsh, *J. Appl. Electrochem.* 28 (1998) 251.
- [22] C. Ponce de León, R.W. Field, *J. Membr. Sci.* 171 (2000) 67.
- [23] C.J. Brown, F.C. Walsh, D. Pletcher, *Trans. I Chem. E* 73 (1995) 196.
- [24] R.K. Raman, N.A. Choudhury, A.K. Shukla, *Electrochim. Solid State Lett.* 7 (2004) A488.
- [25] Z.P. Li, B.H. Liu, K. Arai, S. Suda, *J. Electrochem. Soc.* 150 (2003) A868.